Electronic Supplementary Material (ESI) for Journal of Materials Chemistry A.
This journal is © The Royal Society of Chemistry 2018

Sheet-membrane Mn-doping nickel hydroxide encapsulated via heterogeneous Ni_3S_2 nanoparticles for efficient alkaline battery-supercapacitor hybrid device

Lin Ye‡, Yitong Zhou‡, Zepei Bao‡, Yuguang Zhao, Yining Zou, Lijun Zhao* and Qing Jiang*

Key Laboratory of Automobile Materials, Ministry of Education and School of Materials Science and Engineering, Jilin University, Changchun, 130022, P. R. China

E-mail: lijunzhao@jlu.edu.cn; jiangq@jlu.edu.cn.

‡ These authors contributed equally to this work.

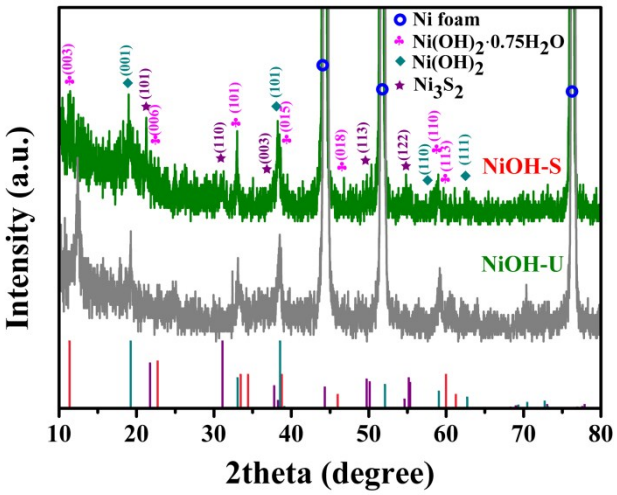

Fig. S1 XRD patterns of NiOH-U and NiOH-S samples

According to the XRD patterns in Fig. S1, we could determine the compositon of NiOH-U and NiOH-S. The NiOH-U is composed of two types of $Ni(OH)_2$ structures (JCPDS no. 38-0715 and 14-0117), and the NiOH-S also contians $Ni(OH)_2$ (JCPDS no. 38-0715 and 14-0117) and Ni_3S_2 (JCPDS no. 44-1418) phases. Compared with NiMn-1 and NiMn-2, the extra $Ni(OH)_2$ (JCPDS no. 14-0117) could form in NiOH-U and NiOH-S. For simplified calculation and fast comparison among NiMn-1, NiMn-2,

NiOH-U and NiOH-S, we still selects the $Ni(OH)_2$ (JCPDS no. 38-0715) and Ni_3S_2 (JCPDS no. 44-1418) to construct molecule models.

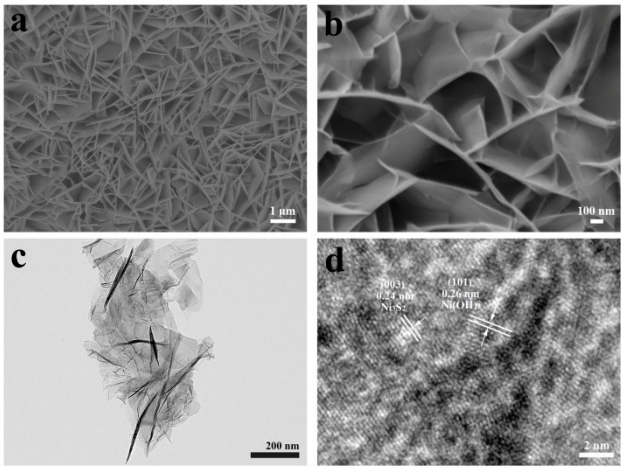

Fig. S2 (a and b) FESEM images of NiMn-2 at low and high magnifications; (c) TEM images of NiMn-2; (e) HRTEM image of NiMn-2.

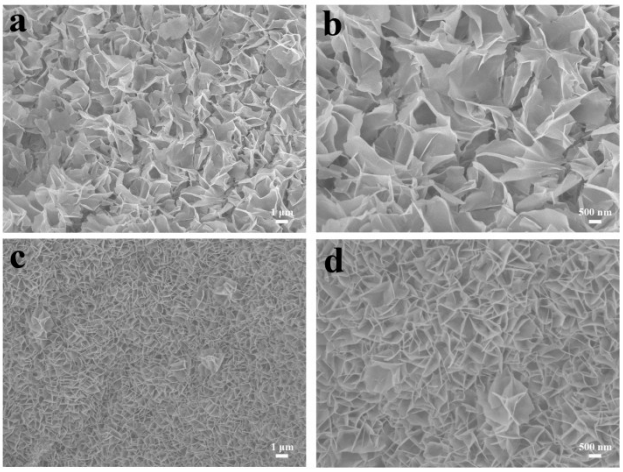

Fig. S3 (a and b) FESEM images of NiOH-U at low and high magnifications; (c and d) FESEM images of NiOH-S at low and high magnifications.

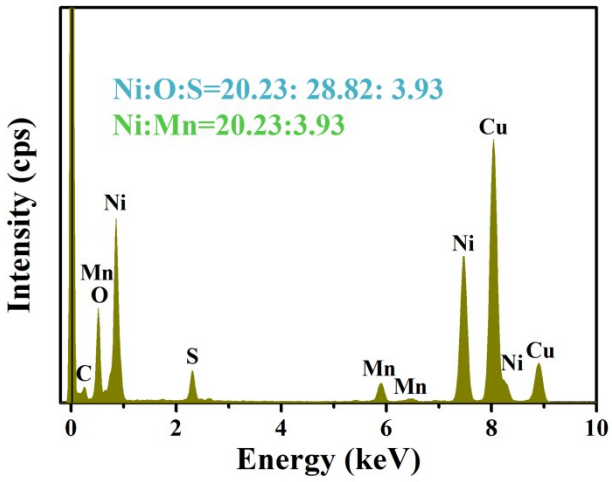

Fig. S4 EDX spectra of NiMn-1

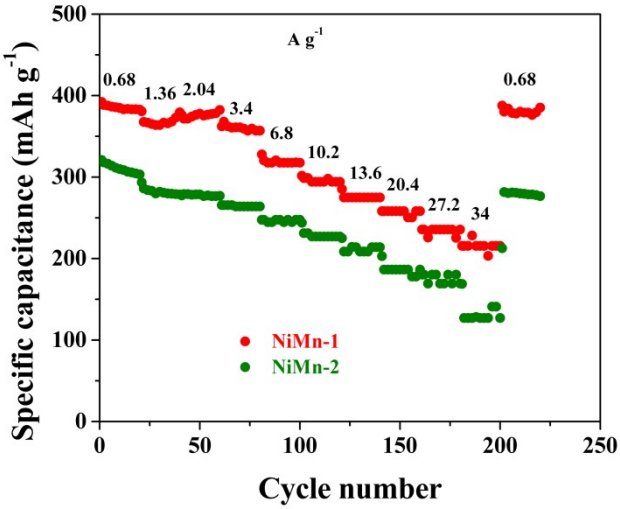

Fig. S5 Cycling measurements of NiMn-1 and NiMn-2 electrodes at different current densities.

For further verifying rate stability of NiMn-1 electrode, we also provide cycling measurements of NiMn-1 and NiMn-2 electrodes at different current densities. In the initial measurements, the NiMn-1 and NiMn-2 electrodes could reach 392.3 mAh g^{-1} (at 0.68 A g^{-1}) and 320.7 mAh g^{-1} (0.68 A g^{-1}), respectively. Meanwhile, the NiMn-1 electrode could reach 215.6 mAh g^{-1} at 34 A g^{-1}, and maintain 387.8 mAh g^{-1} after returning 0.68 A g^{-1}, which

generally coincides well with the rate performance in Fig. 4d. However, the NiMn-2 could only display a capacitance of 127.1 mAh g^{-1} at 34 A g^{-1}. After returning the 0.68 A g^{-1}, the NiMn-2 presents a lower capacitance of 281.6 mAh g^{-1}. Compared with the initial capacitance (in Fig. S5) and rate performance (in Fig. 4d), obvious capacitance fade of NiMn-2 electrode could be found. All these results further demonstrate that NiMn-1 electrode possesses enhanced structure stability.

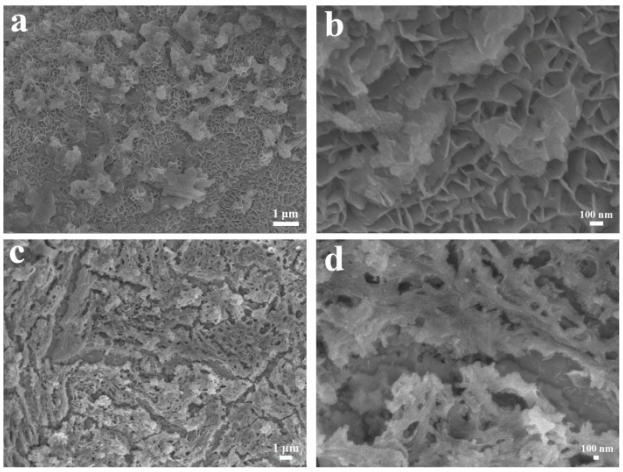

Fig. S6 (a and b) FESEM images of NiMn-1 after 3000 cycles; (c and d) FESEM images of NiMn-2 after 3000 cycles.

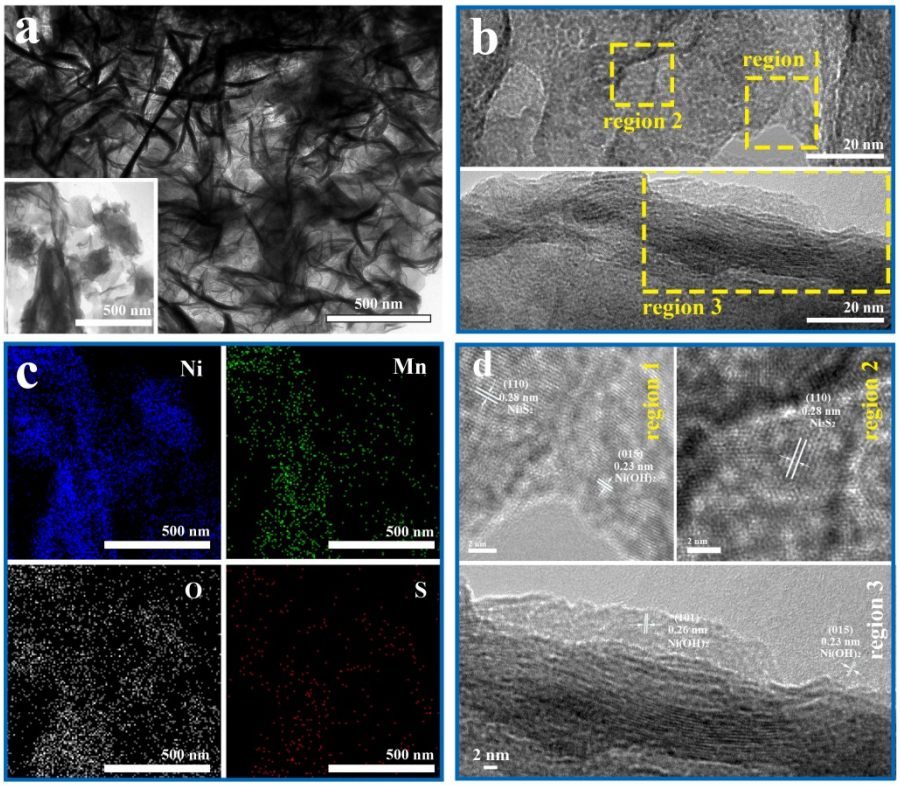

Fig. S7 (a) TEM image of NiMn-1 after 3000 cycles. The inset of S7a is the magnification of circular area; (b) TEM images of NiMn-1 after 3000 cycles at high magnification; (c) elemental mapping of inset area of S7a for NiMn-1 after cycles; (f) HRTEM images of NiMn-1 after cycles from Region 1 to 3.

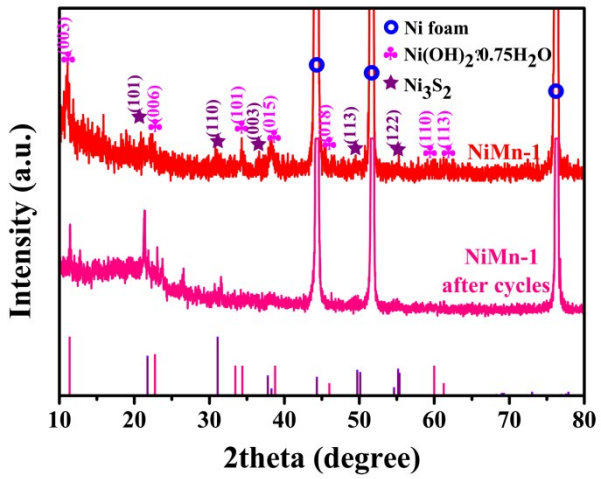

Fig. S8 XRD patterns of NiMn-1 before and after 3000 cycles

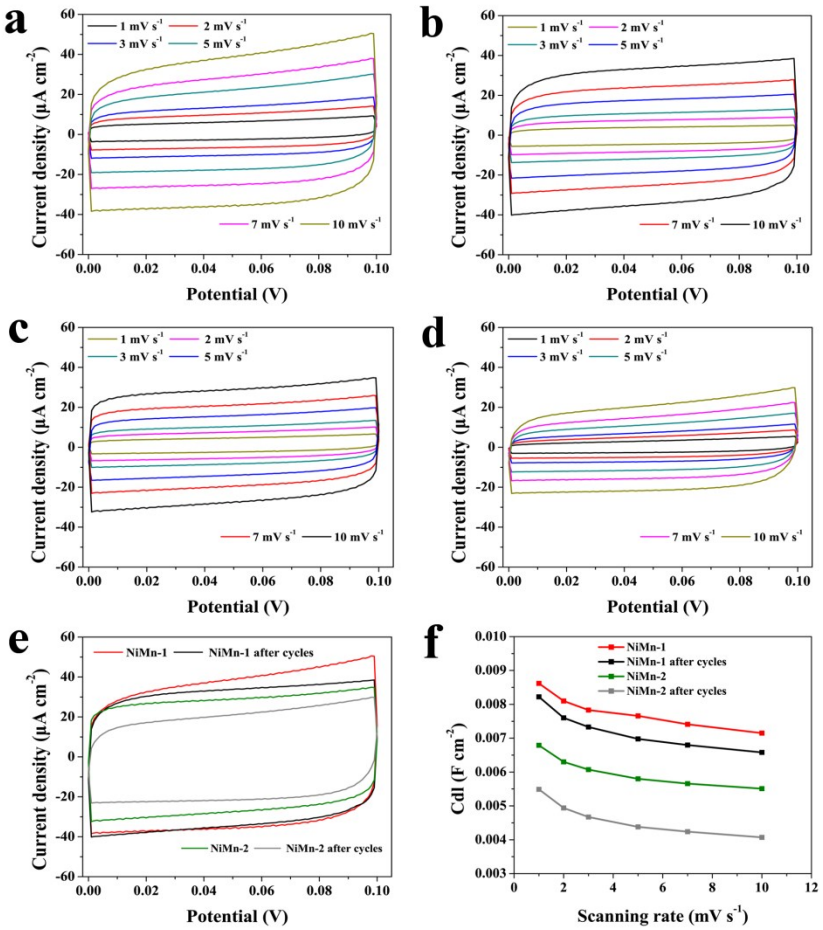

Fig. S9 (a) CV curves of NiMn-1 before cycles in the non-redox area (from 0 to 0.1 V); (b) CV curves of NiMn-1 after cycles in the non-redox area; (c) CV curves of NiMn-2 before cycles in the non-redox area; (d) CV curves of NiMn-1 after cycles in the non-redox area; (e) CV comparison of NiMn-1 and NiMn-2 electrodes before/after cycles; (f) C_{dl} performance of NiMn-1 and NiMn-2 electrodes before/after cycles.

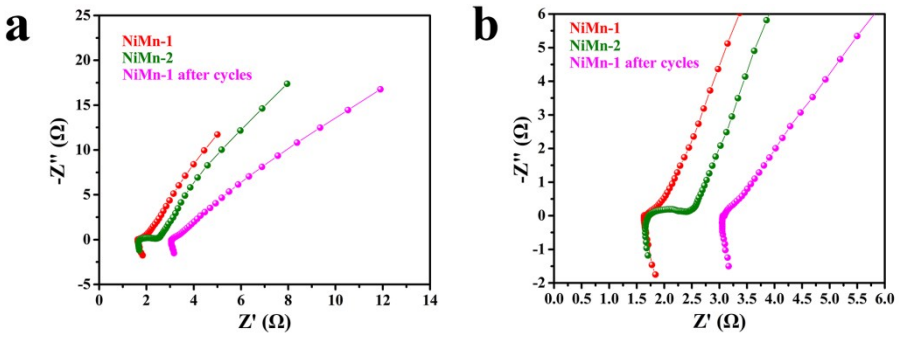

Fig. S10 (a) EIS spectra of NiMn-1 and NiMn-2 electrodes; (b) magnification of EIS spectra with a Z' range from 0 to 6 Ω.

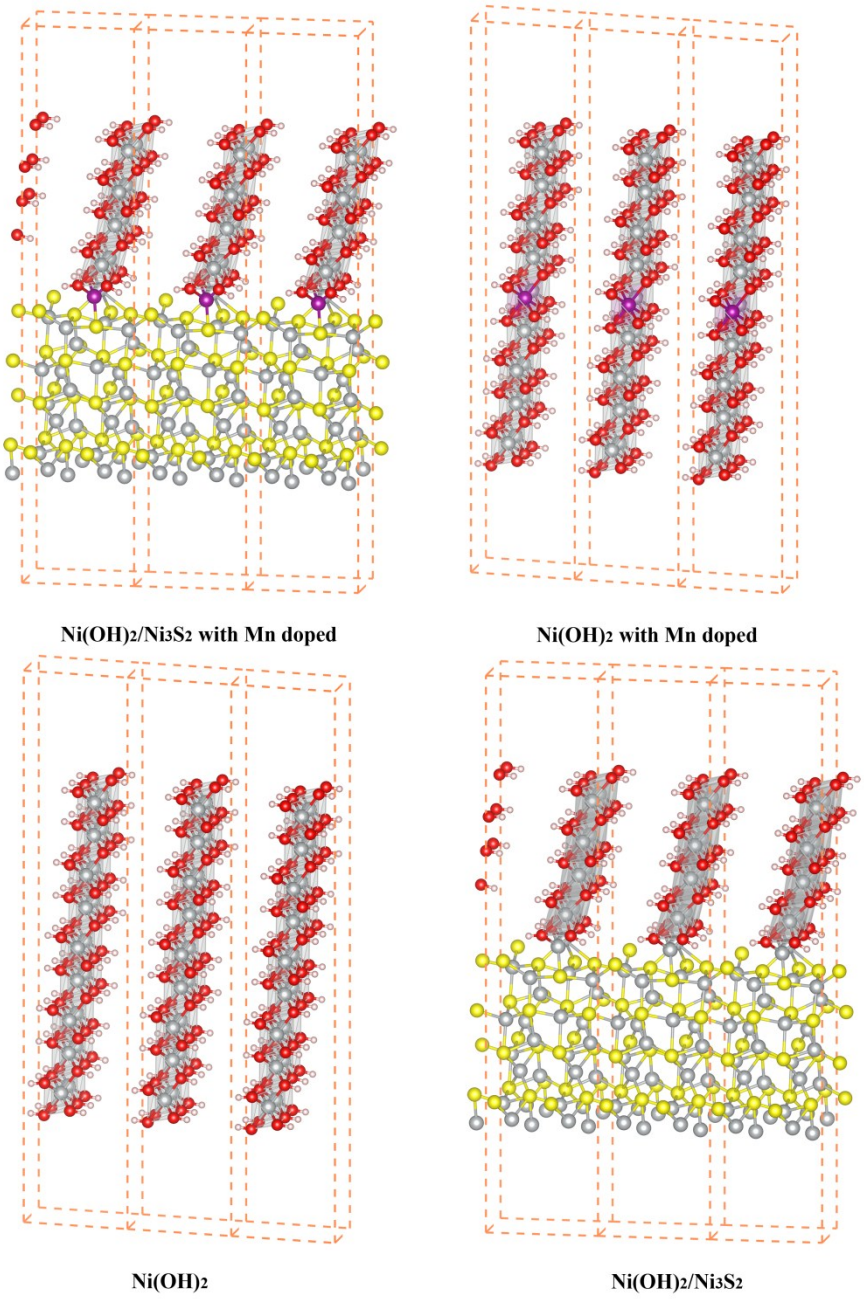

Fig. S11 Various molecule models of $Ni(OH)_2/Ni_3S_2$ with Mn-doping, $Ni(OH)_2$ with Mn-doping, $Ni(OH)_2$ and $Ni(OH)_2/Ni_3S_2$.

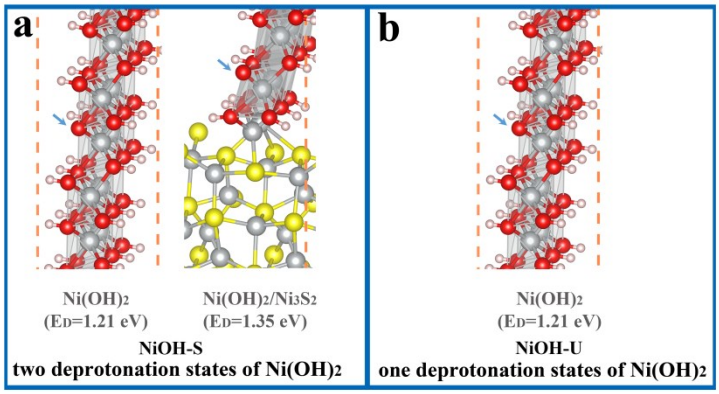

Fig. S12 (a) two deprotonation states of $Ni(OH)_2$ in the NiOH-S; (b) one deprotonation states of $Ni(OH)_2$ in the NiOH-U. The grey, red, light pink and yellow balls represent the Ni, O, H and S atoms.

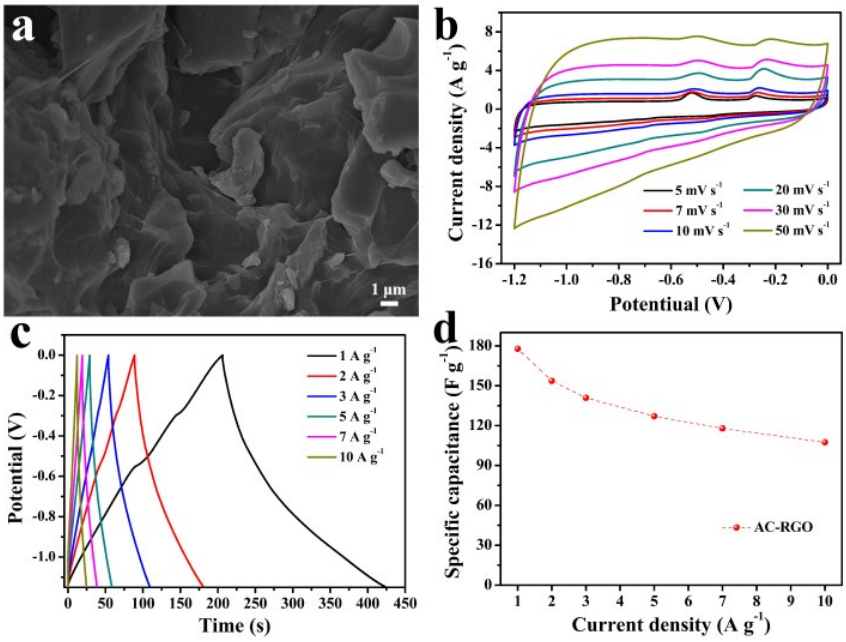

Fig. S13 (a) FESEM image of AC-RGO; (b) (b) CV profiles of AC-RGO electrode at different scanning rate from 5 to 50 mV s^{-1}; (c) GCD profiles of AC-RGO at different current densities from 1 to 10 A g^{-1}; (d) rate performance for AC-RGO electrode 1 to 10 A g^{-1}.

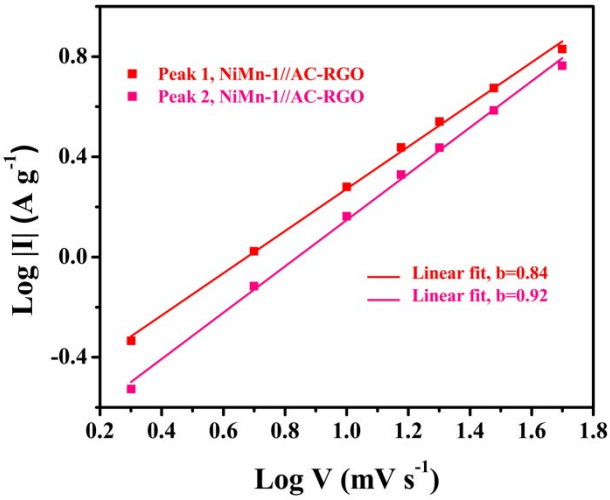

Fig. S14 Log │I│- Log V plots of NiMn-1//AC-RGO (peak 1 and peak 2)